UNIVERSITY OF BIRMINGHAM

University of Birmingham Research at Birmingham

The dielectric properties of some ceramic substrate materials at terahertz frequencies

Ma, Mingsheng; Wang, Yi; Navarro-Cia, Miguel; Liu, Feng; Zhang, Faqiang; Liu, Zhifu; Li, Yongxiang; Hanham, S. M.; Hao, Zhang-cheng

[Link to publication on Research at Birmingham portal](#)

Accepted Manuscript

Title: The Dielectric Properties of Some Ceramic Substrate Materials at Terahertz Frequencies

Authors: Mingsheng Ma, Yi Wang, Miguel Navarro-Cía, Feng Liu, Faqiang Zhang, Zhifu Liu, Yongxiang Li, Stephen M. Hanham, Zhangcheng Hao

Please cite this article as: Ma M, Wang Y, Navarro-Cía M, Liu F, Zhang F, Liu Z, Li Y, Hanham SM, Hao Z, The Dielectric Properties of Some Ceramic Substrate Materials at Terahertz Frequencies, *Journal of the European Ceramic Society* (2019), https://doi.org/10.1016/j.jeurceramsoc.2019.06.012

This is a PDF file of an unedited manuscript that has been accepted for publication. As a service to our customers we are providing this early version of the manuscript. The manuscript will undergo copyediting, typesetting, and review of the resulting proof before it is published in its final form. Please note that during the production process errors may be discovered which could affect the content, and all legal disclaimers that apply to the journal pertain.

The Dielectric Properties of Some Ceramic Substrate Materials at Terahertz Frequencies

Mingsheng Ma[a], Yi Wang[b, *], Miguel Navarro-Cía[c], Feng Liu[a], Faqiang Zhang[a], Zhifu Liu[a, *], Yongxiang Li[d], Stephen M. Hanham[b], Zhangcheng Hao[e]

[a]CAS Key Laboratory of Inorganic Functional Materials and Devices, Shanghai Institute of Ceramics, Chinese Academy of Sciences, Shanghai 200050, P. R. China

[b]Department of Electronic, Electrical and Systems Engineering, University of Birmingham, Birmingham B15 2TT, U. K.

[c]School of Physics and Astronomy, University of Birmingham, Birmingham B15 2TT, U. K.

[d]School of Engineering, RMIT University, Melbourne, VIC 3000, Australia

[e]State Key Laboratory of Millimeter-Waves, School of Information Science and Engineering, Southeast University, Nanjing 210096, China

[*]Corresponding email: y.wang.1@bham.ac.uk; liuzf@mail.sic.ac.cn

Abstract

The terahertz (THz) dielectric constant (ε_r') and dielectric loss tangent (tanδ) of the commercial LTCC materials (Ferro A6M and DuPont 951), Al_2O_3 (ceramic and single crystal), AlN and β-Si_3N_4 ceramics were measured using the vector network analyzer (VNA) over the frequency range of 140-220 GHz and the time-domain spectrometer (TDS) from 0.2 to 1.0 THz. The results from the two instruments are compared with the literatures and show good agreement and consistency. For Ferro A6M, ε_r'=6.06, tanδ=0.012 at 1.0 THz. For DuPont 951, ε_r'=7.67, tanδ=0.097 at 1.0 THz. For Al_2O_3 ceramic and single crystal, the measured THz dielectric properties are consistent with the reported works. The dielectric constant of AlN (ε_r'=8.85) and β-Si_3N_4 (ε_r'=8.41) ceramics at THz region is a little lower than that of the reported values at MHz to GHz region. These results provide valuable and much needed reference information for device designers and material scientists.

***Keywords*:** Dielectric properties; Terahertz band; Ceramic substrate materials

1. Introduction

In recent years, the terahertz (THz) region of the electromagnetic spectrum, referring roughly to the frequencies from 10^{11} to 10^{12} Hz, has attracted significant interest in materials science, communication and biomedical engineering [1-3]. In high frequency electronic applications, multilayer ceramics technology, such as low temperature co-fired ceramics (LTCC) and high temperature co-fired ceramics (HTCC), is considered one promising platform for the development of the emerging THz devices and systems [4, 5]. LTCC and HTCC have been widely used in microwave and millimeter wave devices and packages due to their suitability for low-cost mass production. It is expected that LTCC and HTCC hold equal promises for devices and packaging at THz frequencies. The accurate determination of ceramic dielectric properties in the THz band is a prerequisite for their proper use. However, there is very little information in the open literature about the dielectric properties of materials at these frequencies, and that available shows some inconsistency [6]. This is a major constraint for the development of THz devices, such as antennas, filters, resonators, sensors, as well as for THz packaging using ceramic substrates. Therefore, knowing the THz dielectric properties of the ceramic substrate materials is essential.

The measurement of the dielectric properties of materials in the THz band is most commonly performed using a vector network analyzer (VNA) or a time-domain spectrometer (TDS) [7]. A VNA allows terahertz measurement in the frequency domain and the frequency coverage has been extended to 1.5 THz in recent years using waveguide-based frequency extension modules. The use of waveguide test ports, however, makes the VNA measurements band-limited, but with extremely high frequency resolution on the order of a single hertz. The dielectric properties of the material under test (MUT) reflect the continuous wave response, with the results given in terms of the S-parameters (S_{11} and S_{21}). The TDS is based on the pulsed wave response of the material. It is a wide-band system capable of reaching several THz easily in a single pulse measurement at the expense of frequency resolution, which is of the order of GHz [8]. The TDS system is usually subject to a lower frequency limit of around 200 GHz below which the measurement becomes unreliable due to the drop

in signal-to-noise ratio [8]. Using TDS, the dielectric properties of the MUT can be deduced from a complex numerical Fourier analysis of the reference (without MUT) and MUT response. It is worth mentioning that most of the reported THz dielectric measurements carried out using VNA or TDS were focused on polymers and semiconductors [8, 9]. There is very little such data available for ceramic substrate materials. On the one hand, the low attenuation of the ceramic materials renders very small signal contrast between the measurements with and without the MUT, which increases the error in parameter extraction of the imaginary part of the complex relative permittivity. On the other hand, the relatively high dielectric constant of ceramic materials often causes strong reflection at their interfaces with air, resulting in multiple reflections in the MUT. This complicates the parameter extraction from both the continuous wave and the time-domain pulse measurements. Because of these challenges facing the measurements at THz frequencies for ceramic materials, it is advisable to verify data using different techniques such as the VNA and TDS in order to increase the reliability and fidelity of the results [6].

In this work, the commonly used commercial LTCC materials, Ferro A6M and DuPont 951, and the typical high-temperature sintered ceramic substrate materials, Al_2O_3 (in both ceramic and crystal forms), AlN and β-Si_3N_4 ceramics, were characterized using both VNA and TDS measurements. Using the VNA, the dielectric constant and dielectric loss tangent ($\tan\delta = \varepsilon_r''/\varepsilon_r'$, where ε_r'' and ε_r' are the imaginary and real parts of the complex relative permittivity, respectively) of these selected materials were investigated over the frequency band of 140-220 GHz (WR-05 waveguide band) with a commercially available THz material characterization kit (MCK). The same materials were also measured using the TDS method over a wider frequency range from 0.2 to 1.0 THz. The results from the two methods were compared and cross-checked with each other. These results provide useful reference information for device designers and material scientists.

2. Experimental procedure

The samples tested in this work are several typical inorganic substrate materials

with different compositions and structures. They include the glass-ceramic (Ferro A6M), composite of glass and ceramic (DuPont 951), oxide ceramic (Al_2O_3), crystal (Al_2O_3 crystal along the direction parallel to c-axis), and nitride ceramics (AlN and β-Si_3N_4). The Al_2O_3 (ceramic and crystal), AlN and β-Si_3N_4 samples were produced at Shanghai Institute of Ceramics, Chinese Academy of Sciences (SICCAS). All of the samples were fabricated into circle plates with the same diameter of 20 mm and the thickness of 1 mm.

Figure 1a shows the schematic diagram of the VNA measurement setup. A pair of WR-05 frequency extenders (Virginia Diodes, USA) were connected to the VNA (Agilent N5247A, USA), which enabled the measurements in the WR-05 waveguide band between 140 GHz and 220 GHz. The material characterization kit (MCK, SWISSto12, Switzerland [10]) was used in conjunction with the frequency extenders. The MCK have a waveguide transition from rectangular waveguide to corrugated circular waveguide. This is essentially a mode converter from the TE_{10} mode at the VNA test port to the hybrid Gaussian HE_{11} mode at the output of the MCK. This allows the electromagnetic wave to propagate within an enclosed low-loss environment and form a near-planar wavefront before impinging on the MUT [4]. The sample is inserted between the two corrugated waveguide sections. The material dielectric parameters can be derived from the S-parameters (S_{11} and S_{21}) measured by the VNA based on the following equations [10, 11]:

$$\varepsilon_r^* = \varepsilon_r^{'} - j\varepsilon_r^{"} = \frac{1}{\mu_r^* k_0^2}\left(\frac{4\pi^2}{\Lambda^2} + k_c^2\right) \tag{1}$$

$$\mu_r^* = \mu_r^{'} - j\mu_r^{"} = \frac{2\pi}{\Lambda\sqrt{k_0^2 - k_c^2}}\left(\frac{1+\Gamma}{1-\Gamma}\right) \tag{2}$$

$$\Gamma = X \pm \sqrt{X^2 - 1} \tag{3}$$

$$X = \frac{S_{11}^2 - S_{21}^2 + 1}{2S_{11}} \tag{4}$$

$$\frac{1}{\Lambda^2} = -\left[\frac{1}{2\pi L}\ln(T)\right]^2 \tag{5}$$

$$T = \frac{S_{11} + S_{21} - \Gamma}{1 - (S_{11} + S_{21})\Gamma} \tag{6}$$

where ε_r^* is the complex relative permittivity. The real part (ε_r') is referred to as the dielectric constant, and the imaginary part (ε_r'') is the loss factor. k_c is the cutoff wavenumber and k_0 is the wavenumber in air. μ_r^* is the complex relative permeability. The real part (μ_r') is referred to as the relative permeability, and the imaginary part (μ_r'') is the magnetic loss. Γ is the reflection coefficient. T is the transmission coefficient. L is the thickness of the sample. A standard two-port calibration procedure was carried out at the waveguide ends prior to the measurements. The calculations of the dielectric constant (ε_r') and dielectric loss tangent ($\tan\delta = \varepsilon_r''/\varepsilon_r'$) of the samples were accomplished using SWISSto12 MCK software based on the measured amplitude and phase of S_{11} and S_{21}.

Figure 1b shows the schematic diagram of the TDS measurement setup in a collimated beam configuration whereby the frequency-dependent beam-diameter at the sample position is smaller than 10 mm over the whole frequency band. The time delay of this TDS system (TERA K15 Mark II, MenloSystems, Germany) for the measurements was set to be 143.125 ps, with a 0.3125 ps resolution, resulting in a maximum bandwidth of 3.2 THz and a spectral resolution of ~7 GHz. Given the dynamic range of the system and the samples' absorption coefficient, the measurement bandwidth is smaller than 3.2 THz [8]. To obtain the samples' dielectric properties, the THz signals with and without the sample are compared. The recorded time traces are transferred to the frequency domain using a Fourier transform for spectroscopic evaluation. The frequency-dependent refractive index $n(\omega)$ and extinction coefficients $\kappa(\omega)$, and the real and imaginary parts of the complex relative permittivity (ε_r' and ε_r'') of the sample can be calculated by solving the transfer function of the sample in the frequency domain $H(\omega)$ [12]:

$$\varepsilon_r^* = \varepsilon_r' - j\varepsilon_r'' = (n^2 - \kappa^2) - j(2n\kappa) \tag{7}$$

$$\tan\delta = \frac{\varepsilon_r''}{\varepsilon_r'} = \frac{2n\kappa}{n^2 - \kappa^2} \tag{8}$$

$$H(\omega) = \frac{E_s(\omega)}{E_{\text{ref}}(\omega)} = \frac{4n(\omega)}{\left[n(\omega)+1\right]^2} \cdot e^{-\kappa(\omega)\frac{\omega L}{c}} \cdot e^{-j[n(\omega)]\frac{\omega L}{c}} \cdot FP(L,\omega) \qquad (9)$$

$$FP(L,\omega) = \sum_{i=0}^{\infty} \left[\left(\frac{n(\omega)-1}{n(\omega)+1}\right)^2 \cdot e^{-j2n(\omega)\frac{\omega L}{c}} \right]^i = \frac{1}{1 - \left(\frac{n(\omega)-1}{n(\omega)+1}\right)^2 \cdot e^{-j2n(\omega)\frac{\omega L}{c}}} \qquad (10)$$

where $n(\omega)$ and L are the complex refractive index and thickness of the sample, respectively, c is the speed of the light, and $FP(L,\omega)$ is the Fabry-Perot term that accounts for multiple reflections inside the sample. Under certain assumptions, $n(\omega)$ and $\kappa(\omega)$ (and therefore ε_r' and $\tan\delta$) could have been described by a closed-form solution, but we opted here to evaluate them more accurately via the iterative approach implemented by the TeraLyzer software. The mean absolute deviation for the dielectric constant and dielectric loss tangent was estimated from three consecutive measurements for every sample. The error bars constitute an indication for the statistical errors of the measurement methods of the VNA and TDS.
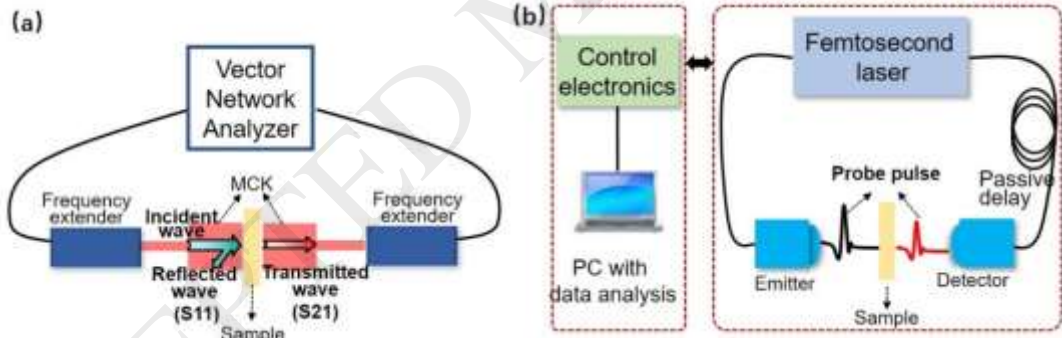
Figure 1. Schematic diagram of the (a) VNA, and (b) TDS measurement setups.

3. Results and Discussion

Figure 2 shows the dielectric properties of the Ferro A6M and DuPont 951 samples measured using the VNA over 140-220 GHz and using the TDS over 0.2-1.0 THz. The dielectric constants (ε_r') of both samples are almost unchanged over the concerned frequency bands. For the overlapping frequency region between 200 and 220 GHz, the results from the VNA and the TDS are in good agreement. The dielectric constants of

both samples measured by the VNA are slightly smaller than those by the TDS. For the sample of Ferro A6M, the dielectric constants from the VNA and TDS are about 5.9 and 6.0, respectively. These are very close to the data declared by the manufacturer (~5.9 @10-100 GHz) [13]. For the sample of DuPont 951, the dielectric constants from the VNA and TDS are about 7.5 and 7.6, respectively. These are also consistent with the value of 7.52 at 90-140 GHz reported in [14]. The dielectric loss tangent (tan δ) of the Ferro A6M is about 0.003 over 140-220 GHz. It is observed that the dielectric loss tangent increases by one order of magnitude to about 0.012 as the frequency increases to 1.0 THz. It is important to note that the dielectric loss tangent of the DuPont 951 is much higher than that of the Ferro A6M. This is mainly due to the different material compositions between the two materials. The Ferro A6M is a glass-ceramic system with high crystallinity, whereas the DuPont 951 is a composite of glass and Al_2O_3. The alkali metal ions with high ionic mobility in the lossy glass of DuPont 951 is responsible for its higher dielectric loss tangent [15].

Figure 2. Dielectric properties of the samples of Ferro A6M and DuPont 951 measured using (a) the VNA, and (b) the TDS.

Figure 3 shows the dielectric properties of Al_2O_3 ceramic and crystal measured using the VNA and TDS. The dielectric constant of Al_2O_3 ceramic fluctuates slightly around 9.3 in the frequency range of 140-220 GHz measured by the VNA. The TDS measurement gives a smooth line of ~9.36 within the frequency band of 0.2-1.0 THz.

It was reported that the dielectric constant of Al_2O_3 ceramic at 1 THz is 9.3 in [16]. For the Al_2O_3 crystal along the direction parallel to c-axis, the dielectric constant is around 11.26 from the VNA over 140-220 GHz, while it shows a smooth line of around 11.4 over 0.2-1.0 THz in the TDS measurements. Previous work reported that the dielectric constant of Al_2O_3 crystal along the direction parallel to c-axis was about 11.3 at a much lower frequency of 24 GHz [17]. The Al_2O_3 crystal has a rhombohedral type structure and is a highly anisotropic crystal, and the dielectric properties are dependent on crystallographic orientation. It has been reported that the dielectric constant of the Al_2O_3 crystal along the direction perpendicular to c-axis is about 9.3, whereas that along the direction parallel to c-axis is about 11.5 at 10^3-10^9 Hz [18, 19]. Since the Al_2O_3 ceramic is composed of polycrystalline Al_2O_3, which are randomly oriented, it is understandable that the Al_2O_3 ceramic shows a dielectric constant value between that of Al_2O_3 crystal along the direction parallel to c-axis and that perpendicular to c-axis direction. The lower dielectric constant in the Al_2O_3 ceramic may be also resulted from pores, voids and sintering aids. It is plausible to assume there are more pores and voids in the polycrystalline Al_2O_3 ceramic than those in the transparent Al_2O_3 single crystal sample. The dielectric loss tangent of the Al_2O_3 ceramic is around 0.003 over 140-220 GHz, and doubles as the frequency increases to 1.0 THz. In contrast, the Al_2O_3 crystal presents very low loss over the entire frequency range of interest. In fact, the loss is so low that the measurement uncertainty renders negative values from the VNA method. This is not unusual for the measurement of low loss materials. Similar behavior was reported in other work using the VNA method [20]. The small fluctuation of the results in Figure 3a is also a signature of the VNA method. This is mainly attributed to the Fabry-Perot resonance due to multiple reflections at the dielectric-air interfaces of the low loss samples [21]. This is only revealed by the high frequency resolution of the VNA measurement. The parameter extraction algorithm cannot deal with the Fabry-Perot resonance as effectively for very low loss materials as for higher loss materials. It can also be observed that the lower loss Al_2O_3 crystal sample shows larger fluctuation in the measured results. Compared to the Al_2O_3 crystal, the higher dielectric loss tangent of the Al_2O_3 ceramic is believed to be largely due to the scattering of THz waves by the

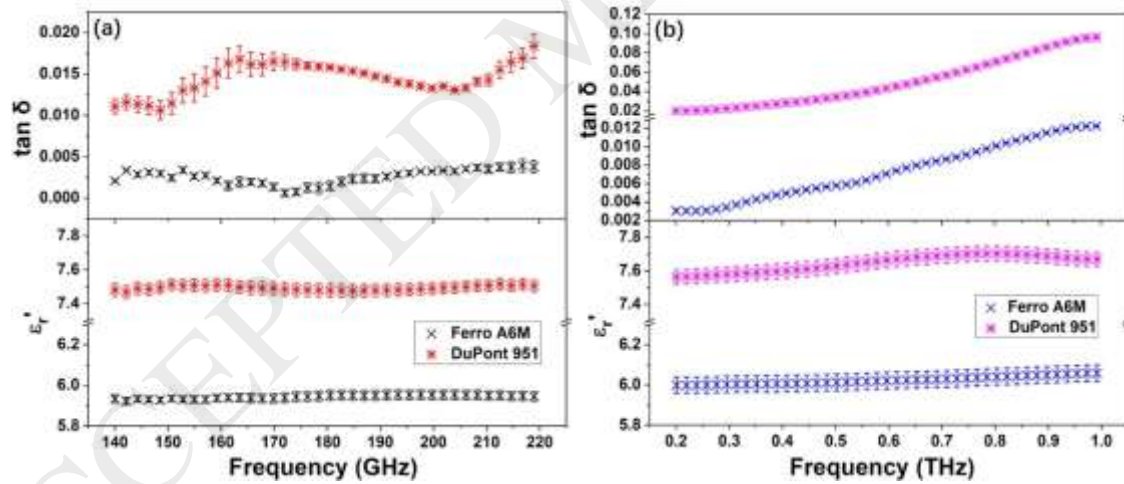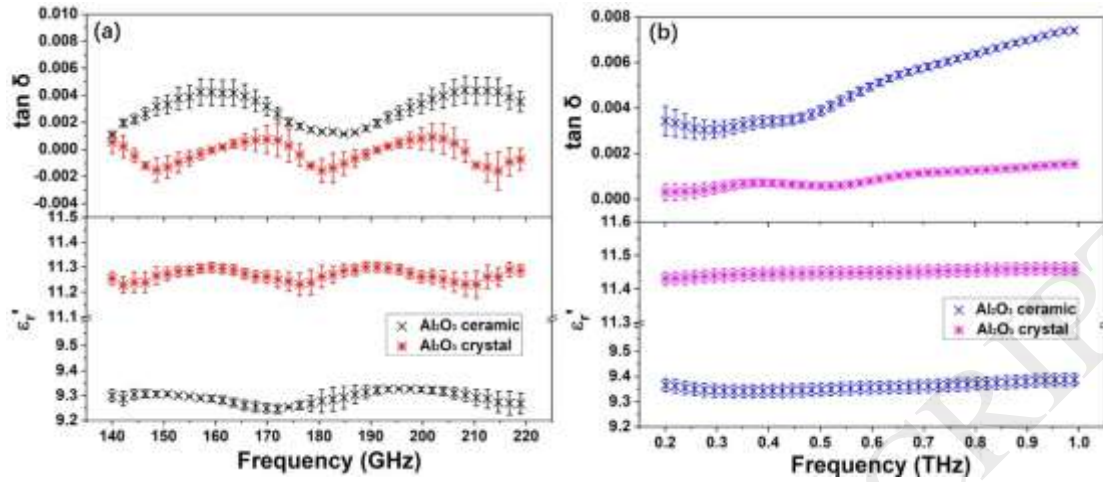grain boundaries and possible voids in the polycrystal Al_2O_3 ceramic [22].

Figure 3. Dielectric properties of the Al_2O_3 ceramic and crystal measured using (a) the VNA, and (b) the TDS.

Figure 4 shows the dielectric properties of AlN and Si_3N_4 ceramics measured using the VNA and TDS. The dielectric constant of AlN ceramic is around 8.7~8.8 in the frequency of 140-220 GHz, and almost unchanged (~8.83) from 0.2 to 1.0 THz. The dielectric constant of Si_3N_4 ceramic is around 8.3~8.4 in the frequency of 140-220 GHz and almost unchanged (~8.43) from 0.2 to 1.0 THz. It is worth mentioning that the dielectric constants of both the AlN and Si_3N_4 ceramics are somehow smaller than previously reported results in MHz or GHz regions [23, 24]. The reasons are as follows: the dielectric constant of solid materials is related to its polarizability, which is frequency dependent. In general, polarizability is the combined contribution from dipolar orientational polarization, ionic displacement polarization and electron displacement polarization, which requires 10^{-10}~10^{-12} s, 10^{-12}~10^{-13} s and 10^{-14}~10^{-15} s to form the polarization, respectively. In the MHz or GHz region, the dielectric constant is attributed to the sum of all three polarizations. While in the THz region, there is insufficient time to allow for the formation of the dipolar orientation polarization, and thus the dipolar orientation polarization drops out. It is believed that the polarization is mainly attributed to ionic displacement and electron displacement [25]. Therefore, it is expected that the dielectric constant at THz frequencies is smaller than that at MHz or

GHz. A lower dielectric loss tangent of about 0.001~0.002 is observed in the AlN ceramic than in the Si_3N_4 ceramic. This indicates a better transparency to THz radiation. Si_3N_4 ceramic presents a dielectric loss tangent of about 0.005 in the frequency of 140-220 GHz, and it increases in the THz band. This can be attributed to the scattering of THz waves by the pores and voids in the Si_3N_4 ceramic. Similar to Figure 3, small fluctuations in the results from the VNA measurement are observed.
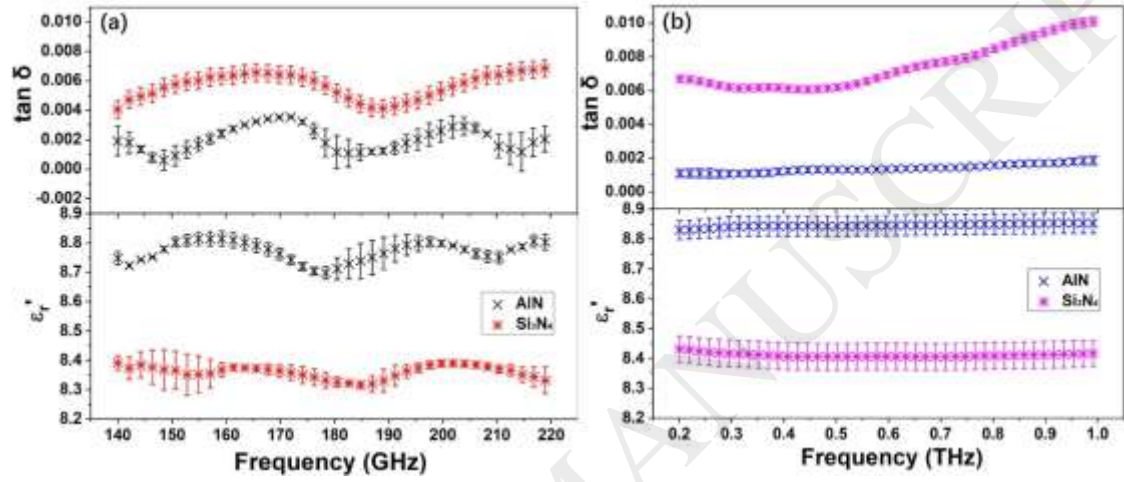

Figure 4. Dielectric properties of the AlN and Si_3N_4 ceramics measured using (a) the VNA, and (b) the TDS.

Table 1 summarizes the results obtained from both the VNA and the TDS method. For comparisons, the data at the overlapping frequency of 200 GHz from both methods are selected. Data from open literatures are also listed in Table 1. Some of them were read from the graphs in the literature. It is evident that the dielectric properties obtained in this work are consistent with most of those available in the literature. Apart from the different sample thickness and test frequency, the differences between our results and the literature may be attributed to the factors such as measurement setup, extraction processes, surface roughness of the samples, and differences in sample manufacturing. It should be mentioned that the measurement uncertainty increases with a reducing thickness of the sample, especially for the low loss samples. The consistency between our results and the literature, together with the good agreement between the VNA and TDS method, provides high confidence in the reliability and accuracy of our data.

Table 1. The results obtained by this work and reported in literatures

Samples	VNA (200 GHz)		TDS (200 GHz)		TDS (1.0 THz)		Literatures		
	ε'_r	tan δ	ε'_r	tan δ	ε'_r	tan δ	ε'_r	tan δ	Ref
Ferro A6M	5.95	0.003	5.99	0.003	6.06	0.012	5.9 @100GHz	0.002 @100GHz	[13]
DuPont 951	7.49	0.014	7.56	0.019	7.67	0.097	7.52 @140GHz	0.01 @140GHz	[14]
Al₂O₃ ceramic	9.32	0.003	9.36	0.003	9.39	0.007	9.3 @1.0 THz	0.003 @1.0 THz	[16]
							9.63 @200GHz	0.0019 @200GHz	[26]
							9.42 @1.0 THz	-	[27]
							9.61 @1.0 THz	-	[28]
							9.28 @1.0 THz	0.004 @1.0 THz	[29]
Al₂O₃ crystal	11.26	0.0008	11.42	0.0003	11.47	0.002	11.3 @24GHz	-	[17]
							11.59 @200GHz	0.0006 @200GHz	[26]
							11.63 @1.0 THz	-	[30]
AlN ceramic	8.79	0.002	8.83	0.001	8.85	0.002	8.9 @ 1MHz	0.0008 @ 1MHz	[23]
							8.296 @96.5GHz	0.00038 @96.5GHz	[31]
							8.4 @1.0 THz	0.001 @1.0 THz	[32]
							8.53 @1.0 THz	-	[33]
Si₃N₄ ceramic	8.38	0.005	8.43	0.006	8.41	0.01	8.5 @ 4GHz	0.003 @ 4GHz	[24]
							(Si₃N₄ thin film) 7.6 @1.0 THz	(Si₃N₄ thin film) 0.005 @1.0 THz	[34]

4. Conclusions

The THz dielectric properties of the commonly used ceramic substrate materials, including Ferro A6M, DuPont 951, Al₂O₃ (both in ceramic and single crystal forms), AlN and β-Si₃N₄ ceramics, were measured using both the VNA (140 ~ 220 GHz) and TDS (0.2 ~ 1.0 THz) instruments. The principles of the measurements were introduced. The good agreement between the two methods confirm the reliability of the measurements. In addition, the dielectric properties obtained in this work are also consistent with most of those available in the literature. This demonstrates that the data we obtained are reliable and accurate. Our results provide valuable and much needed

reference information for the device designers and material researchers at THz frequencies.

References

[1] T. Nagatsuma, G. Ducournau, C. C. Renaud, Advances in terahertz communications accelerated by photonics, Nat. Photonics. 10 (2016) 371-379.

[2] C. Y. Yu, Y. Zeng, B. Yang, R. Donnan, J. B. Huang, Z. X. Xiong, A. Mahajan, B. G. Shi, H. T. Ye, R. Binions, N. V. Tarakina, M. J. Reece, H. X. Yan,. Titanium Dioxide Engineered for Near-dispersionless High Terahertz Permittivity and Ultra-low-loss. Sci. Rep. 7 (2017) 6639.

[3] G. Carpintero, L. E. García Muñoz, H. Hartnagel, S. Preu, A. Räisänen, Semiconductor TeraHertz Technology: Devices and Systems at Room Temperature Operation. Wiley-IEEE Press, (2015).

[4] H. J. Song, Packages for terahertz electronics, P. IEEE, 105 (2017) 1121-1138.

[5] T. Tajima, H. J. Song, M. Yaita, Compact THz LTCC Receiver Module for 300 GHz Wireless Communications, IEEE Microw. Wirel. Comp. 26 (2016) 291-293.

[6] M. Naftaly, An international intercomparison of THz time-domain spectrometers, 41st International Conference on Infrared, Millimeter, and Terahertz waves (IRMMW-THz), DOI: 10.1109/IRMMW-THz.2016.7758763, (2016).

[7] M. Naftaly, R. G.Clarke, D. A. Humphreys, N. M. Ridler, Metrology State-of-the-Art and Challenges in Broadband Phase-Sensitive Terahertz Measurements, P. IEEE, 105 (2017) 1151-1165.

[8] M. Naftaly, Terahertz Metrology, Artech House, (2014).

[9] T. Chang, X. S. Zhang, X. X. Zhang, H. L. Cui, Accurate determination of dielectric permittivity of polymers from 75 GHz to 1.6 THz using both S-parameters and transmission spectroscopy, Appl. Optics. 56 (2017) 3287-3292.

[10] http://www.swissto12.com/products/MCK/.

[11] A. M. Nicholson, G. F. Ross, Measurement of the intrinsic properties of and materials by time domain techniques, IEEE Trans. Instrum. Meas. 19 (1970) 377-382.

[12] W. Withayachumankul, Engineering aspects of terahertz time-domain spectroscopy, PhD dissertation of University of Adelaide. (2009)

[13] https://www.ferro.com/-/media/files/resources/electronic-materials/ferro-electronic-materials-a6m-e-ltcc-tape-system.pdf.

[14] P. R. Bajurko, Millimeter wave permittivity and loss tangent measurements of LTCC materials. 21st International Conference on Microwave, Radar and Wireless Communications (MIKON), (2016), DOI: 10.1109/MIKON.2016.7492104

[15] M. T. Sebastian, R. Ubic, H. Jantunen, Low-loss dielectric ceramic materials and their properties, *Int. Mater. Rev*. 60 (2015) 392-412.

[16] J. A. Hejase, P. R. Paladhi, P. Chahal, Terahertz characterization of dielectric substrates for component design and nondestructive evaluation of packages, IEEE Trans. Comp. Pack. Man. 1 (2011) 1685-1694.

[17] J. Krupka, R.G. Geyer, M. Kuhn, J. H. Hinken, Dielectric properties of single crystals of Al_2O_3, $LaAlO_3$, $NdGaO_3$, $SrTiO_3$, MgO at cryogenic temperatures, IEEE Trans. Microw. Theory Techn., 42 (1994) 1886-1890.

[18] https://global.kyocera.com/prdct/fc/product/pdf/s_c_sapphire.pdf.

[19] H. Tang, H. Li, J. Xu, Growth and development of sapphire crystal for LED applications, Advanced Topics on Crystal Growth. IntechOpen, 2013.

[20] A. Khalid, D. Cumming, R. Clarke, C. Li, N. Ridler, Evaluation of a VNA-based material characterization kit at frequencies from 0.75 THz to 1.1 THz, IEEE 9th UK-Europe-China Workshop on Millimetre Waves and Terahertz Technologies (UCMMT). 2016, DOI: 10.1109/UCMMT.2016.7873952.

[21] W. Sun, B. Yang, X. Wang, Y. Zhang, R. S. Donnan, Accurate determination of terahertz optical constants by vector network analyzer of Fabry-Perot response, Opt. Lett. 38 (2013) 5438-5441.

[22] J. D. Breeze, J. M. Perkins, D. W. McComb, N. M. Alford, Do Grain Boundaries Affect Microwave Dielectric Loss in Oxides? J. Am. Ceram. Soc. 92 (2009) 671-674.

[23] N. Kuramoto, T. Taniguchi, I. Aso, Translucent A1N ceramic substrate, IEEE Trans. Comp. Pack. Man. 9 (1986) 386-390

[24] J. Barta, M. Manela, R. Fischer, Si_3N_4 and Si_2N_2O for high performance radomes, Mater. Sci. Eng. A. 71 (1985) 265–272.

[25] S. Wang, Q. Li, J. Q. Gu, J. G. Han, W. L. Zhang, Dielectric properties of MgO–ZnO–TiO_2 based ceramics at 1 MHz and THz frequencies, J. Mater. Sci. 52 (2017) 9335-9343.

[26] M. N. Afsar, Precision Millimeter-Wave Dielectric Measurements of Birefringent Crystalline Sapphire and Ceramic Alumina, IEEE Trans. Instrum. Meas. 36 (1987) 554-559.

[27] Y. Kim, M. Yi, B. G. Kim, J. Ahn, Investigation of THz birefringence measurement and calculation in Al_2O_3 and $LiNbO_3$, Appl. Opt. 50 (2011) 2906-2910.

[28] A. K. Klein, J. Hammler, C. Balocco, A. J. Gallant, Machinable ceramic for high performance and compact THz optical components, Opt. Mat. Express 8 (2018) 1968-1975.

[29] P. H. Bolivar, M. Brucherseifer, J. G. Rivas, R. Gonzalo, I. Ederra, A. L. Reynolds, M. Holker, and P. Maagt, Measurement of the dielectric constant and loss tangent of high dielectric-constant materials at terahertz frequencies, IEEE Trans. Microw. Theory Techn., 51 (2003) 1062-1066.

[30] D. Grischkowsky, S. Keiding, M. V. Exter, C. Fattinger, Far-infrared time-domain spectroscopy with terahertz beams of dielectrics and semiconductors, J. Opt. Soc. Am. B. 7 (1990) 2006-2015.

[31] B. Komiyama, M. Kiyokawa, and T. Matsui, Open Resonator for Precision Dielectric Measurements in the 100 GHz Band, IEEE Trans. Microw. Theory Techn., 39 (1991) 1792-1796.

[32] S. B. Kang, D. C. Chung, S. J. Kim, J. K. Chung, S. Y. Park, K. C. Kim, M. H. Kwak, Terahertz characterization of Y_2O_3-added AlN ceramics, Appl. Surf. Sci. 388 (2016) 741-745.

[33] M. Naftaly, P. J. Greenslade, R. E. Miles, and D. Evans, Low loss nitride ceramics for terahertz windows, Opt. Mater. 31 (2009) 1575-1577.

[34] G. Cataldo, J. A. Beall, H. M. Cho, B. McAndrew, M. D. Niemack, E. J. Wollack，Infrared dielectric properties of low-stress silicon nitride, Opt. Lett. 37 (2012) 4200-4202.